

APPLICATION OF ATTENUATED TOTAL REFLECTION
SPECTROSCOPY TO FUSED INORGANIC SALTS

By

ALAN RAY BANDY

Bachelor of Arts

Oklahoma State University

Stillwater, Oklahoma

1964

Submitted to the faculty of the Graduate School of
the Oklahoma State University
in partial fulfillment of the requirements
for the degree of
MASTER OF SCIENCE
August, 1964

JAN 8 1955

APPLICATION OF ATTENUATED TOTAL REFLECTION

SPECTROSCOPY TO FUSED INORGANIC SALTS

Thesis Approved:

J. Paul Dowlin

Thesis Adviser

Tom E. Moore

J. W. Boyce

Dean of the Graduate School

570110

ACKNOWLEDGMENT

The author wishes to thank his thesis adviser, Dr. J. Paul Devlin, who has contributed much to the content of this thesis.

This work has been possible, in large part, by financial support from the National Science Foundation and the Oklahoma State University Research Foundation.

Thanks must also go to the machinists, who constructed the foreoptics and to Dr. J. Fahrenfort, who made available detailed drawings of the foreoptics.

TABLE OF CONTENTS

Chapter	Page
I. INTRODUCTION	1
II. ATTENUATED TOTAL REFLECTION SPECTROSCOPY	4
III. APPLICATION OF ATR TO FUSED SALTS	6
IV. INSTRUMENTATION	8
V. EXPERIMENTAL	13
VI. RESULTS	17
VII. DISCUSSION	19
BIBLIOGRAPHY	30

LIST OF ILLUSTRATIONS

Figure	Page
1. A Family of Curves Relating Reflecting Power to n and μ at a Given Incident Angle	22
2. Diagram of Foreoptics	23
3. Back View of Angle Dividing Mechanism	24
4. Foreoptics and Monochromator	24
5. Diagram of Sample Cell	25
6. ATR Spectra of Lithium Nitrate	26
7. ATR Spectra of Lithium Nitrate	27

LIST OF PLATES

Plate	Page
I. Infrared Spectrum of Ultrapure Silicon	28
II. Foreoptics	29

CHAPTER I

INTRODUCTION

Until recently research in fused salts has been stimulated by problems which arise in extractive electrolysis; however, interest is increasing in the synthetic chemistry and coordination chemistry of molten salts and in their potential in catalysis of organic reactions.

Since a knowledge of the structure of fused salts is essential to the advancement of their chemistry, such physiochemical studies as electrical transport, viscosity, phase change calorimetry, and cryoscopy have been directed toward structural problems common to molten salt systems.

If the ionic interactions in a fused salt are sufficiently intense, the influence of the environment on the chemical species present may be spectroscopically observable. Further, one might expect to obtain information concerning the degree of covalent interaction, the extent of local order, and the existence of complex ions in an inorganic molten salt from the vibrational spectrum of that fused salt system.

Bues^{1,2} has used Raman spectroscopy to study the Raman active modes of certain fused nitrates. However, neither Raman nor infrared absorption techniques alone can ordinarily yield the complete vibrational spectrum; they should be used to compliment each other. Infrared and Raman can be employed as a check on one another, or one spectrum can be used to locate the vibrational modes which are inactive in the other. However, there is no assurance that the lines observed in the Raman arise

from the same chemical species as those bands which are observed in the infrared.

The experimental problems which arise in the Raman spectroscopy of fused salts are fewer in number and less severe than those which arise in infrared transmission spectroscopy. These problems in the Raman technique have been discussed by Bues³.

The corrosive nature of fused salt systems limits the use of ordinary infrared window materials. Thus, infrared transmission spectroscopy is difficult to apply since suitable corrosion resistant materials which transmit over the proper wavelength range, 2 to 50 μ , and over the desired temperature range, are rare. The only material which is known to have the above properties is type II diamond which is quite expensive. Pure silicon transmits from 2 to 50 μ , but reflection losses become critical at the longer wavelengths; also, silicon becomes metallic, and thus opaque, at approximately 375^o C.

In general fused inorganic salts are highly absorbing substances. Consequently, a sample thickness of 10 μ or less is often necessary. A sample thickness of this order is difficult to prepare, measure, and control. Greenberg and Hallgren⁴ have avoided the infrared window problem by suspending the fused salt on a platinum wire screen and passing the radiation directly through the fused sample. Here however, the sample thickness is too great for the very intense bands which occur in fused salts.

Wilmschurst and Senderoff⁵ have sidestepped both the window and pathlength problems by measuring the reflection spectrum from the bare fused salt surface. The absorption spectrum was then calculated from the reflection spectrum by utilizing the Robinson and Price⁶ method

for analyzing reflection data. This technique also yields the refractive indices and the absorption indices as a function of frequency. The chief disadvantage is the tedious calculations which are required to analyze reflection data and the high probability of significant errors in the wing corrections which has been discussed by Schatz and Plaskett⁷.

As was mentioned in the preceding paragraph the vibrational spectrum of a fused salt can be calculated from the reflection spectrum from the bare fused salt surface. However, if the bare surface of the salt is covered by a prism of transparent material, then total internal reflection will occur at the prism salt interface at frequencies for which the sample is nonabsorbing, the refractive index of the sample is less than the refractive index of the prism material, and the angle of incidence is greater than the critical angle. At frequencies where the medium becomes absorbing, total internal reflection will not occur as the reflected beam will be attenuated. This causes the spectrum of the reflected radiation to appear much as an absorption spectrum. Fahrenfort^{8,9} has concluded that the ATR spectrum of a substance is very similar to its transmission absorption spectrum under certain well defined conditions. The purpose of this investigation was to develop methods whereby the absorption spectrum of a fused salt could be obtained in a routine manner without tedious calculations and with a sample sufficiently thin to yield the spectra of even the very intense bands of inorganic molten salt systems. ATR, which gives a sample penetration from 0.10 to 1 wavelength of the radiation used, has been shown to be a suitable basis for such a method.

CHAPTER II

ATTENUATED TOTAL REFLECTION SPECTROSCOPY

Fahrenfort⁸ has emphasized that the ratio of the reflected amplitude to the incident amplitude, $R(\theta, n, \kappa, \nu)$, for light reflected from the surface of a substance is dependent on the refractive index of the sample, n , the absorption index of the sample, κ , and the incident angle, θ . Consequently, the reflected amplitude is a function of frequency, because the absorption and refractive indices are functions of frequency. Fahrenfort and Visser⁹ has proposed a method whereby one measures the reflecting power for each frequency at two different incident angles, and thus obtains two equations in the two unknowns, κ , the absorption index, and n , the refractive index. These two equations may be solved simultaneously to yield the optical constants n and κ at each frequency.

In measuring band centers, however, such an analysis is unnecessary in attenuated total reflection work provided one chooses the proper conditions. As was mentioned earlier, in ATR no energy is taken from the incident light beam if the incident angle is greater than the critical angle, provided the sample is nonabsorbing. Although total internal reflection occurs the light beam actually penetrates a short distance, somewhat less than one wavelength, into the sample medium. The amplitude of the radiation decreases exponentially in the sample medium thus giving a sample penetration of less than two times the wavelength of the light. The actual effective sample penetration is strongly dependent

on the angle of incidence and the ATR prism index of refraction. However, at frequencies where the sample becomes absorbing total internal reflection will not occur and energy will be removed from the light beam. If the resulting ATR spectra are to be similar to absorption spectra, the reflecting power must be constant with respect to refractive index and dependent only upon the absorption index. To achieve this, the proper prism material must be chosen as well as the proper incident angle. Fahrenfort⁹ has graphed families of curves (Figure 1) showing reflecting power versus refractive index for a specific incident angle and a fixed absorption index. According to these curves one can see that for an incident angle of 48° the reflecting power is very nearly a function of κ alone if the relative refractive index, $n(\text{sample})/n(\text{prism})$, is less than 0.73. Therefore, if the relative refractive index remains less than 0.73 over the entire range of frequencies that is of interest, then ATR spectra should closely resemble transmission spectra although the band shapes may be somewhat altered.

The conventional reflection method cannot be successfully applied to substances whose absorption index is less than 0.02 and which have a refractive index in the interval $1 < n < 2$, because the reflecting power is almost invariant with respect to the absorption index; therefore, reliable values for the optical constants are difficult to calculate under these conditions. Although this is usually not relevant to fused salt work, since fused salts are usually highly absorbing, it should be noted that this difficulty with weak bands does not exist in the ATR technique.

CHAPTER III

APPLICATION OF ATR TO FUSED SALTS

The fact that fused salts are very corrosive and highly absorbing compounds, as mentioned in the introduction, makes the measurement of their transmission spectrum difficult. The choice of transparent inert window materials is extremely limited and the very short sample thickness which is required is difficult to prepare and control.

The magnitude of these experimental difficulties is greatly reduced if the ATR technique is applied. This technique gives a sample thickness of less than $10\ \mu$ which is sufficiently thin to permit observation of the most intense bands of fused salts. It also eliminates reflection problems inherent in absorption work as well as problems in infrared cell assembly. However, the problem of a suitable prism material is still a very real one. Fortunately, ultrapure silicon, which is inert to molten nitrates, chlorates, perchlorates, and halides (except fluorides) also possesses the other properties necessary in an ATR window. Ultrapure silicon transmits about 100 percent of the unreflected light at a wavelength of $5\ \mu$. However, about 30 percent of the light is reflected from each interface where total internal reflection does not occur. Silicon, as is evident in Plate I, is reasonably transparent from 2.5 to $50\ \mu$, but reflection losses become critical at long wavelengths. Unfortunately silicon does become metallic, and thus opaque, at approximately 375°C and is somewhat reactive with fluorides, nitrites, and hydroxides.

The silicon used in this work was semiconductor grade silicon purchased

from Texas Instrument Corporation. The silicon had a resistivity greater than 600 ohm-centimeter.

CHAPTER IV

INSTRUMENTATION

The foreoptics for the reflection measurements (Plate II) are similar to the foreoptics used by Fahrenfort⁸. A cell mount (A) has been added which will support the brass cell (B) containing the fused salt. The mount has adjustments which allow the cell to be raised or lowered vertically and rotated in a plane parallel to the base of the foreoptics. These adjustments allow the sample and silicon prism to be positioned at the focus of a spherical mirror (M_1) such that a maximum amount of radiation will traverse the optical train.

Figure 2 is a diagram of the foreoptics. Infrared radiation originating from a globar source (S) is chopped at (C), reflected from the spherical mirror (M_1), again from the plane mirror (M_2), and then enters the sample cell through a small window. The radiation passes through one side of the silicon prism (P) and is totally internally reflected from its bottom surface. The radiation then leaves the cell through another window whereupon it is reflected by the plane mirror (M_3), then the spherical mirror (M_4), and directed into the monochromator slits by a plane mirror (M_5).

An angle dividing mechanism was employed to control the incident angle of the radiation impinging on the sample. In Plate II the two mirrors (M_1) and (M_2), the source (S), and the chopper assembly (D) are mounted on a magnesium plate (E) which can be moved horizontally along tracks (F) and (G) by a screw mechanism (H). As the screw moves

the magnesium plate (E) horizontally, the mirrors (M_2) and (M_3) rotate and the sample cell (B) and cell mount (A) move along two circular tracks (I) and (J). This mechanism is necessary to keep the radiation focused on the sample while the angle of incidence is being changed. The mirrors (M_2) and (M_3) are mounted on steel shafts (Figure 3-A and B) which extend through the magnesium base plate (Plate II-E). These shafts are rigidly attached to two flat steel arms (Figure 3-C and D). Slots were cut in the ends of the arms and were used to pivot the arms on a shaft (Figure 3-E) which extends from the cell mount through a large hole cut in the magnesium base plate. As the screw is turned the shaft connected to the mirror (M_2) translates horizontally. Because of the manner in which the arms (Figure 3-C and D) are pivoted the mirrors (M_2) and (M_3) are rotated as the shaft to mirror (M_2) translates. The position of the pivot also moves with the cell mount.

The foreoptics are contained in a large wooden dry box. The front and one side of the dry box was constructed from plexiglass to insure ample visibility of the sample in the sample cell. A small plexiglass door was incorporated into the plexiglass front and sealed with a neoprene gasket and screws. The door permits the sample cell to be inserted and removed from the foreoptics. An inlet (Figure 4-A) and an outlet (Figure 4-B) for dry air was fitted into the foreoptics box. A large air pump was used to recirculate the dry air through the foreoptics box having forced the air leaving the box through a column of molecular sieve of type 5-A. This process removes large amounts of the atmospheric water and carbon dioxide. Dry nitrogen was used to hold a positive pressure on the foreoptics box and to sweep out the monochromator. The nitrogen enters the monochromator through an inlet in its base and since a brass

tube connects the monochromator and the foreoptics box, the nitrogen can pass into the foreoptics box if the slits are open. The nitrogen leaves the foreoptics box through a small valve in the side of the box. This method of flushing seemed to be satisfactory only when the molecular sieve was regenerated and the leaks in the foreoptics box as well as the dry air recycling system had been minimized. Under these conditions flushing was found to be sufficiently complete in about 30 minutes.

A Perkin-Elmer 12-C Spectrometer with sodium chloride optics was used. The base of the monochromator was sawed in two immediately in front of the monochromator housing, and the source assembly was removed and bolted into position on the movable magnesium platform of the ATR foreoptics. Three aluminum legs (Figure 4-C) supported the monochromator on a steel plate and allowed it to be adjusted and leveled vertically. The steel plate (Figure 4-D) was bolted to the base of the monochromator with four bolts which pass through slots cut into the steel plate. The existence of these slots allows the monochromator to be adjusted horizontally. A large hole was cut into the steel plate to allow access to the components beneath the monochromator.

The ATR sample cell was machined from brass. This cell contained the crucible of fused salt on an adjustable platform. A prism holder and silicon prism were attached to the end of a micrometer (Figure 5-G) which is extended into the cell by a short piece of ceramic material. This ceramic material prevented heat from being conducted away from the sample and the silicon prism and up the stem of the micrometer. The micrometer screw itself (Figure 5-F) was used to position the silicon prism precisely within the cell.

The cell window, when used, were sodium chloride. They were sealed with glyptal and baked slowly to 150° C to secure from slippage

and leakage. The glass connection (Figure 5-K) was used to evacuate the cell when desired. The cell could be evacuated to about 10μ of mercury.

The crucible shown in Figure 5-A was machined from pure nickel, because fused nitrates of silver, potassium, sodium, and lithium have no apparent corrosive effect on this material. Two loops of 24 gauge nichrome resistance wire was used as a heating element built into the walls of the crucible using fishbone insulators and Sauereisen low expansion cement. Two electrical leads (Figure 5-D) carry the current for the heating element. A hole 0.25 inch in diameter was drilled into the bottom of the crucible. A thermocouple with an insulator 0.25 inch in diameter was wedged in this hole with thin sheets of lead foil. All electrical leads entered the cell via a ceramic leadthrough (Figure 5-D). The crucible was supported on the crucible platform (Figure 5-B) by three small glass beads which insulate the crucible from the platform. An o-ring gasket (Figure 5-E) permitted the cell to be sealed vacuum tight. A screw (Figure 5-1) is used to raise and lower the crucible in such a way that the depth of the prism in the fused salt can be easily controlled without reorienting the silicon prism in the optical path.

Two silicon prisms were used. One prism with a 120° apex angle was machined by Connecticut Instrument Company. Another prism with a 100° apex angle was machined in the laboratory. The prisms were ground on a glass plate using 150, 400, and 600 mesh silicon carbide until the surfaces of the prism were flat and relatively smooth. Then they were polished to a high lustre with cerium oxide on either a taffeta polishing cloth or slick white paper.

Wilmhurst and Senderoff⁵ have reported the maximum refractive index of lithium nitrate to be approximately 2.2. Since silicon has an average

refractive index of 3.6, the maximum critical angle, given by the relation $\sin\theta = n' \sin\phi$, is approximately 37° where ϕ is the angle of refraction, 90° at the critical angle, and n' is the relative refractive index. Consequently, data obtained using the 100° prism is more accurate than from the 120° prism, because the incident angle can be adjusted so that it will always be greater than the maximum critical angle. If the angle of incidence becomes less than the critical angle, it is quite possible that the ATR spectrum will depend to a large extent on changes in the refractive index (e.g. see Figure 1). Since large changes in refractive index occur during an absorption band, distortion of the band is likely to occur.

CHAPTER V

EXPERIMENTAL

Bakers Analyzed Reagent Grade Lithium Nitrate was used without further purification except for drying. This is easily justified in this work where the effective pathlength through the sample is of the order of one micron.

The first acceptable spectrum to be measured is shown in Figure 6-A. The lithium nitrate was dried and otherwise prepared for sampling in the following manner. First, it was placed in the sample cell crucible and left fused in the air for approximately 15 minutes thus removing most of the adsorbed water and gases. The salt was then solidified and the crucible was covered with an aluminum cover to prevent spattering of the cell windows and silicon prism when the sample cell containing the fused salt was evacuated. After being assembled the sample cell was placed in the optical path. The adjustments on the cell mount were employed to maximize the transmitted radiation. Forty-five per cent transmission was recorded with a gain of 17.5, response of 1, a frequency of 3890 cm^{-1} , and a slit of $25\ \mu$.

After the lithium nitrate was fused once again under atmospheric conditions, the sample cell was slowly evacuated. If the cell was evacuated too quickly, violent popping and spattering occurred and solid lithium nitrate soon appeared on the cell windows as was indicated by a very intense band at 1390 cm^{-1} . The liquid salt was left under a vacuum of $60\ \mu$ for 2 hours. Considerable bumping occurred, but no solid or liquid

appeared in the background spectrum which was run during this period after water vapor and carbon dioxide absorption were reduced to a minimum by the flushing procedure mentioned earlier. No attempt was made to heat the silicon prism during the measurement of the background spectrum except by radiation from the aluminum crucible cover.

The salt was then solidified and the sample cell removed from the foreoptics and disassembled. After removal of the aluminum crucible cover the sample cell was reassembled and repositioned in the foreoptics. Again the lithium nitrate was fused. The wavelength control was set at 1390 cm^{-1} , presumably on the band corresponding to ν_3 , the E' asymmetric stretching mode of the nitrate ion. The slit was adjusted until the recorder read 90 per cent transmission, then the crucible was raised until the salt came in contact with the bottom of the silicon prism. The exact depth of the prism was chosen so that further immersion would not result in a decrease in energy. The minimum energy occurred at 55 per cent transmission. The atmospheric carbon dioxide and water absorption was reduced by flushing until it closely matched the intensities of the water and carbon dioxide absorption in the background spectrum. The ATR spectrum was then measured from 3900 cm^{-1} to 1200 cm^{-1} . The extended range of frequencies was chosen in an attempt to check for impurities.

The spectrum was plotted by taking an intensity reading from the spectrum every $1/160$ of a drumnumber. This spectrum was recorded at gain 17.5, response 1, slit $96\ \mu$, and speed 4. The graph in Figure 6-A is a plot of reflecting power versus wavelength in microns for this measurement.

Following the first measurement the background was found to depend on the temperature since more electrons in the silicon crystal attain in energy comparable to the energy difference between the valence band and

the conduction band as the temperature is increased. Subsequently, the silicon prism was placed directly in contact with the crucible cover when the background spectrum was being measured. This procedure brought the silicon prism temperature close to that which it attained during sampling. Also the aluminum crucible cover was replaced by a nickel cover in an attempt to eliminate a possible source of impurities. Except for the above refinements, the spectrum shown in Figure 6-B was obtained in a similar manner as the spectrum shown in Figure 6-A. Both spectra were measured using the 120° prism with an incident angle of 33° . This incident angle is considerably below the maximum critical angle of 37° found in the range of frequencies of the band corresponding to the ν_3 asymmetric stretching vibration of the nitrate ion. Hence a distortion in this band can be expected at those frequencies near the maximum in the sample refractive index. This band distortion was eliminated in a subsequent study by exchanging for a 100° prism. Several other important modifications in technique were also suggested by these original measurements. For example, the spectra in Figure 7-A, 7-B, and 7-C were measured with the cell windows removed, because of the desire to eliminate any possibility of including the absorption spectrum of condensed lithium nitrate with the ATR spectrum of the liquid lithium nitrate. Then, in order to fuse the lithium nitrate without spattering the mirrors (M_2) and (M_3) (Plate II) the lithium nitrate had to be carefully pre-dried. For this purpose a heating plate was constructed inside a pyrex desiccator. One hundred grams of lithium nitrate was placed in a 100 milliliter nickel crucible and fused on the hot plate inside the desiccator. A radiation shield made from aluminum foil was placed around the crucible and freshly dried activated alumina was placed in the bottom of the desiccator. Then the desiccator was sealed and

evacuated to about 100 μ of mercury. The desiccator had to be evacuated very slowly in order to prevent violent bumping. After 2 hours under a vacuum in the fused state the lithium nitrate was assumed to be dry, since no further bumping was detected. It was then allowed to solidify and was stored under a vacuum until used.

Further, since the steel prism holder showed signs of corrosion with the molten lithium nitrate, it was replaced by a nickel holder. Also, during these three runs the prism was checked before and after immersion in the fused salt to ascertain whether or not a thin film of fused lithium nitrate was forming on the two sides of the silicon prism. Such a film would add some absorption spectrum to the ATR spectrum of the liquid. No film was observed.

The base line was determined after the spectrum of the fused salt in case some lithium nitrate had condensed on the mirrors (M_2) and (M_3). During the measurement of the background the silicon prism was placed in direct contact with the bottom of the nickel crucible and thus was heated to the sampling temperature. The spectra in Figures 7-A, 7-B, and 7-C were obtained at 270° C, 300° C, and 315° C respectively.

CHAPTER VI

RESULTS

The free nitrate ion belongs to the D_{3h} symmetry point group. Although there are six fundamental modes of vibration two two-fold degeneracies reduce the number of unique fundamental frequencies to four which have the species $\Gamma = A_1' + 2E' + A_2''$. The A_1' completely symmetric stretching mode of the nitrate ion, ν_1 , has been assigned to a very intense Raman band occurring at 1050 cm^{-1} by Wilmshurst and Senderoff⁵. These workers have also assigned the doubly degenerate E' asymmetric stretching mode, ν_3 , of the nitrate ion to a very intense infrared band and a moderately intense Raman line which occurs at about 1390 cm^{-1} . The E' bending mode and the A_2'' bending mode were assigned to bands occurring at 720 cm^{-1} and 830 cm^{-1} respectively.

The ν_3 stretching frequency was the only band above 1200 cm^{-1} which was sufficiently intense to be detected by the ATR method. The failure to detect the other bands illustrates the very short effective sample thickness achieved by the ATR technique. However, the other bands can be obtained if one resorts to multiple reflection from the salt-silicon interface⁹. In the three spectra in Figure 7 the ν_3 fundamental appears to be split into three bands. The bands occur at approximately 1415 cm^{-1} , 1350 cm^{-1} and 1290 cm^{-1} as compared to 1460 cm^{-1} and 1375 cm^{-1} reported by Wilmshurst and Senderoff⁵. However, these two spectra were both obtained from samples which showed signs of impurities and it is very possible that there is some distortion due to the dependency of the two

spectra on the refractive index. As has been mentioned, this is likely since the critical angle was greater than the 33° incident angle over part of the band. In the last three spectra (Figure 7) the index of refraction effect was minimized, since the 100° silicon prism was used giving an incident angle above the maximum critical angle at all wavelengths. The use of the 100° silicon prism seemed to sharpen and symmetrize the spectrum considerably. Greater regard for sample purity was also exercised; consequently, these three spectra are considered to be superior spectra of lithium nitrate. It can be noted that they indicate band centers at 1410 cm^{-1} , 1335 cm^{-1} , and 1290 cm^{-1} and a slight broadening in the bands as the temperature is increased.

It has been mentioned that three bands were observed where earlier studies have revealed only two bands. This result can be compared to a recent Raman spectrum of molten silver nitrate reported by Walrafen and Irish¹⁰. They found three Raman lines in this region where earlier workers reported only two. This is a good indication that the resolution attained by earlier workers was not sufficient and the complications involved in their experimental procedure and data analysis was too great.

CHAPTER VII

DISCUSSION

Greenberg and Hallgren⁴ have assigned a band occurring at 1061 cm^{-1} to the A'_1 stretching mode of the nitrate ion. For the unperturbed nitrate ion this mode should be Raman active only; however, its appearance in the infrared spectrum of Greenberg and Hallgren⁴ is an indication that the nitrate ion in this environment is perturbed by the cation field such that a symmetry lower than D_{3h} results. This could also account for the splitting of the ν_3 fundamental since it is doubly degenerate only when the C_3 axis is preserved. For example no splitting of the ν_3 fundamental has been observed in the fused potassium nitrate spectrum indicating that the polarizing power of a potassium ion is not great enough to destroy the three-fold symmetry axis of the nitrate ion and thus remove this degeneracy. However, the nitrate group in methyl nitrate belongs to the C_{2v} symmetry point group since the C-O covalent bond reduces the symmetry. Here the E' asymmetric stretch of the free nitrate ion is no longer degenerate. Thus, two bands are observed instead of one. These facts can be used to interpret the above spectra of lithium nitrate. If there were only two bands, they could easily be explained in terms of the polarization of the nitrate ion by the lithium cation causing a reduction in symmetry and thus removal of the degeneracy in the ν_3 fundamental, but the presence of three bands is not completely explained by this point of view. Janz, Kozlowski, and Wait¹¹ have concluded that the trend to lower values for the ν_1 stretching frequency of a series of metal salts can be used as an index

for covalency. This conclusion was drawn from a study of the infrared spectra of a series of solid transition metal salts measured by Gatehouse, Livingstone, and Nyholm¹². Further, Walrafen and Irish¹⁰ report asymmetry in the corresponding Raman band for molten silver nitrate. This asymmetry may result from the addition of two bands, one produced by a covalently associated nitrate group and one by the free ion. Accepting this premise, one can then assign the three lines in the ν_3 portion of the spectrum to bonded nitrate, the strong lines at 1290 cm^{-1} and 1420 cm^{-1} , and the free ion, the weak line at 1350 cm^{-1} . Since silver ion, like the potassium ion, has a low polarizing power, the degeneracy in ν_3 for the free ion is not removed.

One can look at lithium nitrate in much the same manner except the cation is high in polarizing power and, on Janz's¹¹ scale, has a low index of covalency; thus one expects and observes, that the central ν_3 band at 1335 cm^{-1} , assigned to the free ion by analogy with silver nitrate, should be much stronger than in silver nitrate, since ionization should be more nearly complete. Further, no asymmetry in the ν_1 infrared band (or Raman line) has been observed with molten lithium nitrate. This is agreeable, since such asymmetry would indicate the presence of large quantities of covalently bonded nitrate. Admittedly, a splitting in the 1335 cm^{-1} band of the free ion might be expected since lithium ion has a high polarizing power and one might predict the destruction of the three-fold axis in the free nitrate ion as observed in the solid state for lithium nitrate. However, no such splitting has been confirmed in the spectrum of any molten salt.

Thus, both the silver nitrate and lithium nitrate spectra can be satisfactorily explained if one assumes the presence of both free nitrate

ion and covalently bonded nitrate in each case, with the covalent form dominant in silver nitrate and the free ion prevalent in lithium nitrate.

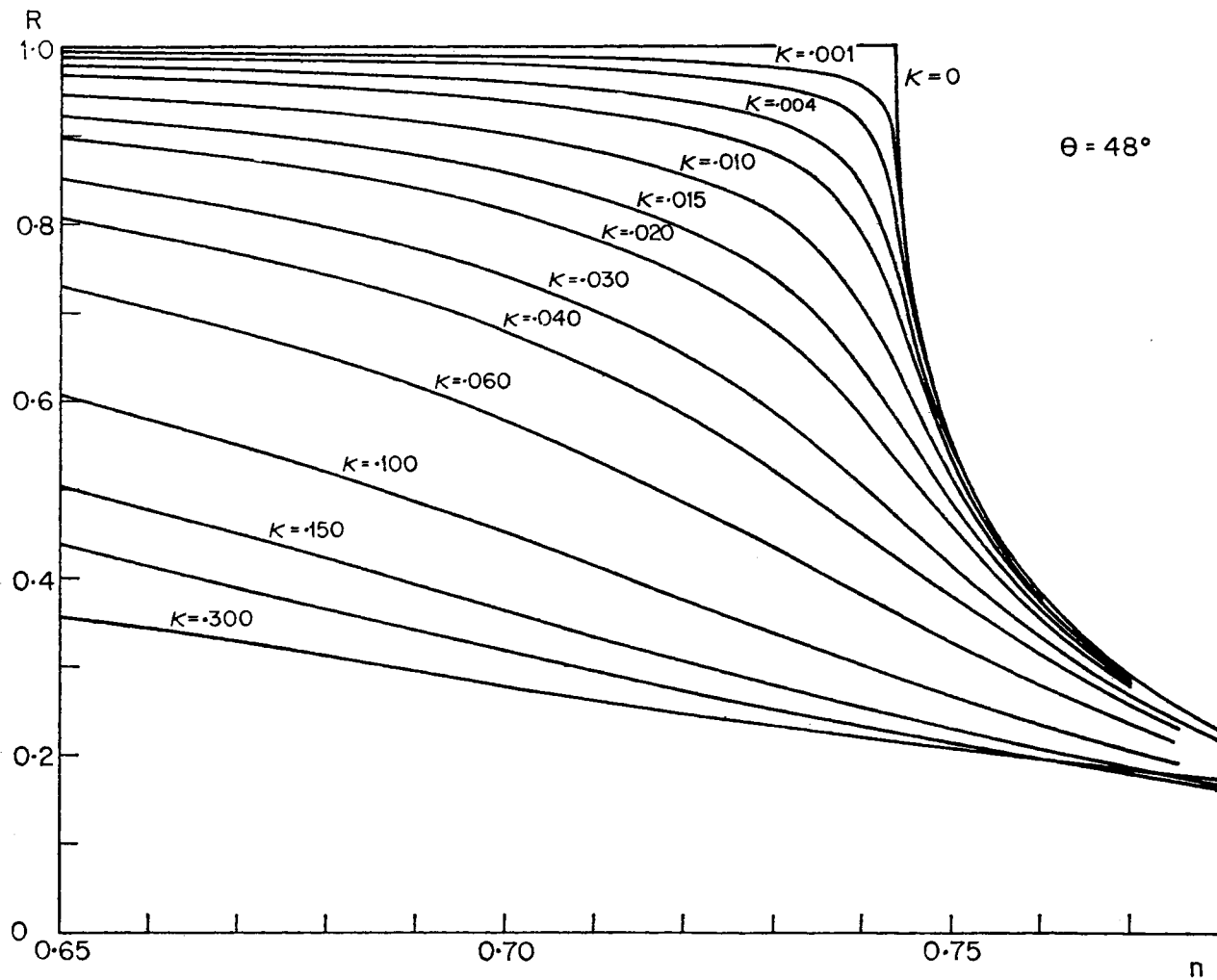


Figure 1. A Family of Curves Relating Reflecting Power to n and K at a Given Incident Angle.

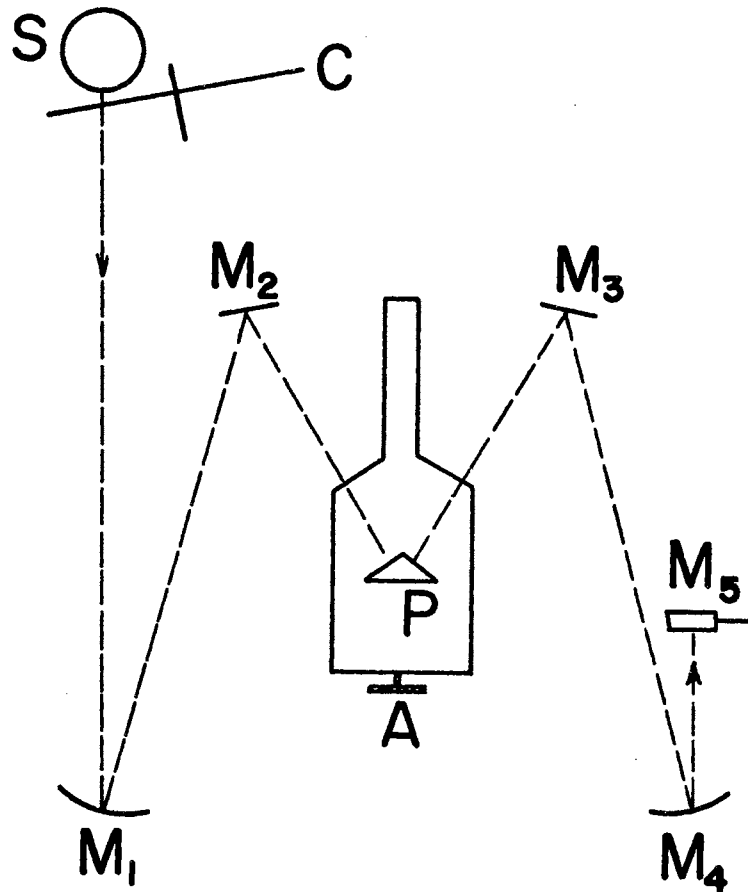


Figure 2. Diagram of Foreoptics.

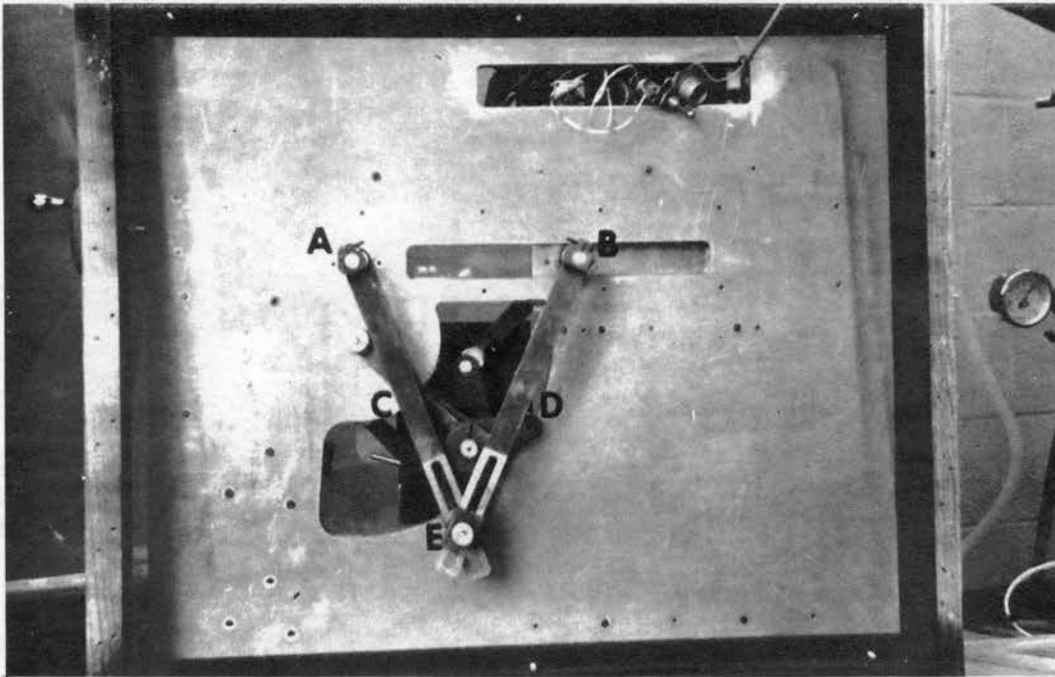


Figure 3. Back View of Angle Dividing Mechanism.

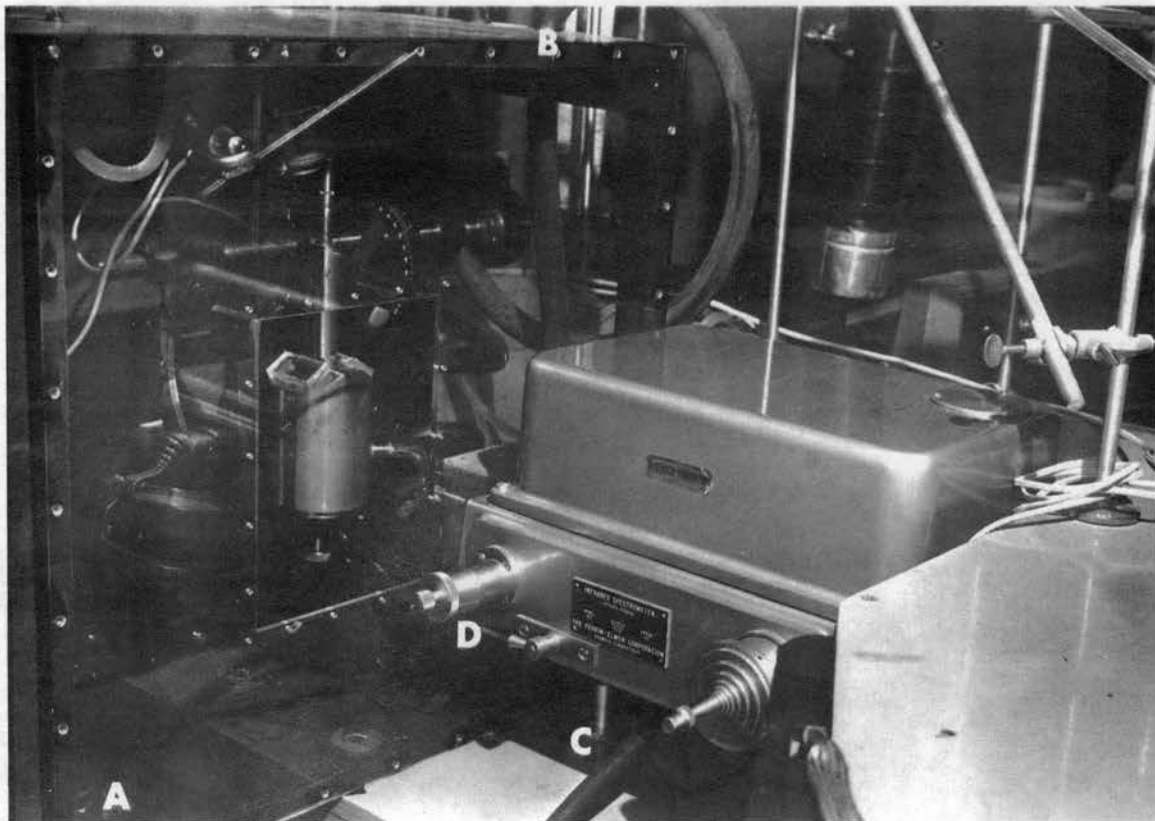


Figure 4. Monochromator and Foreoptics.

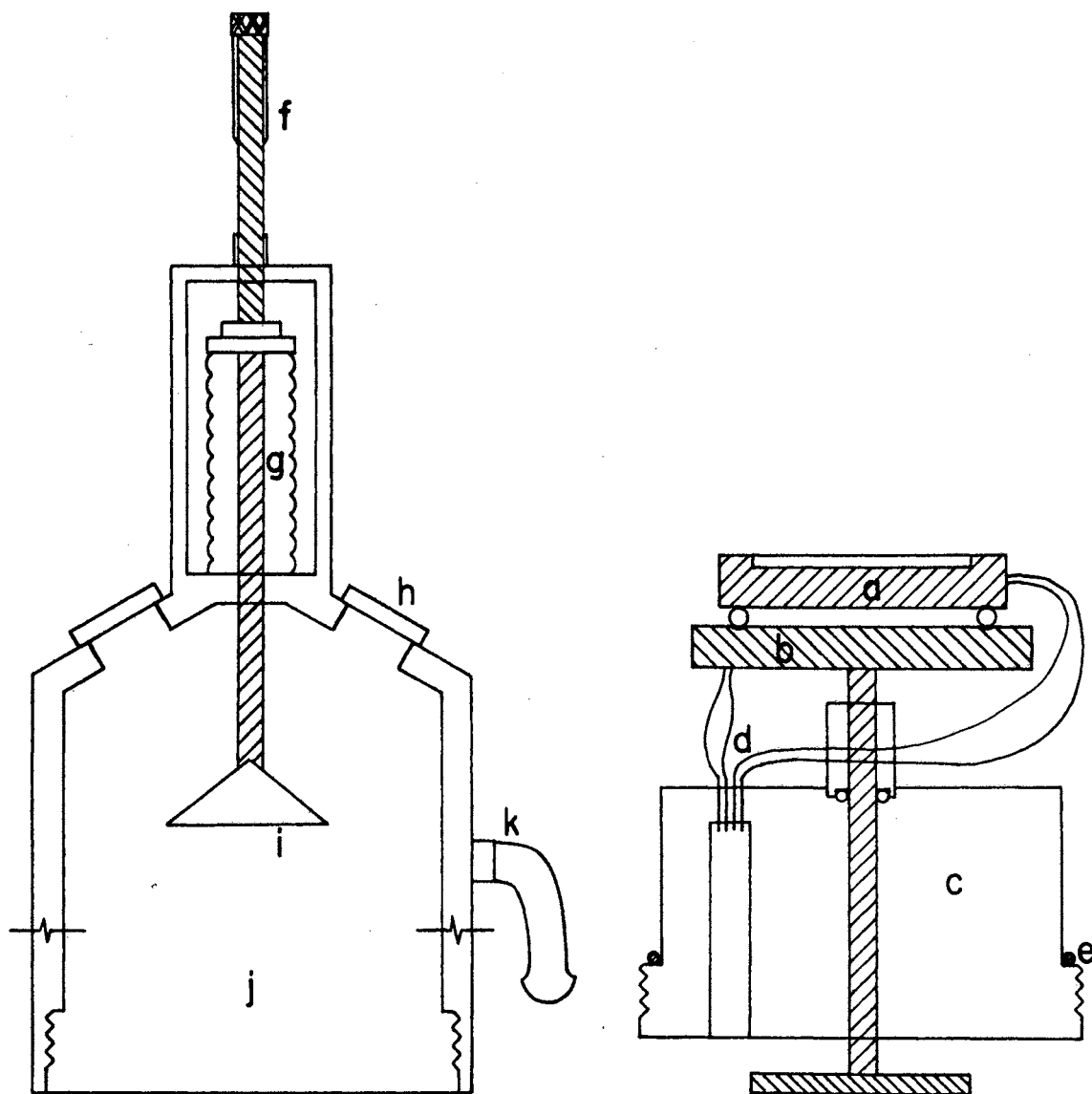


Figure 5. Sample Cell

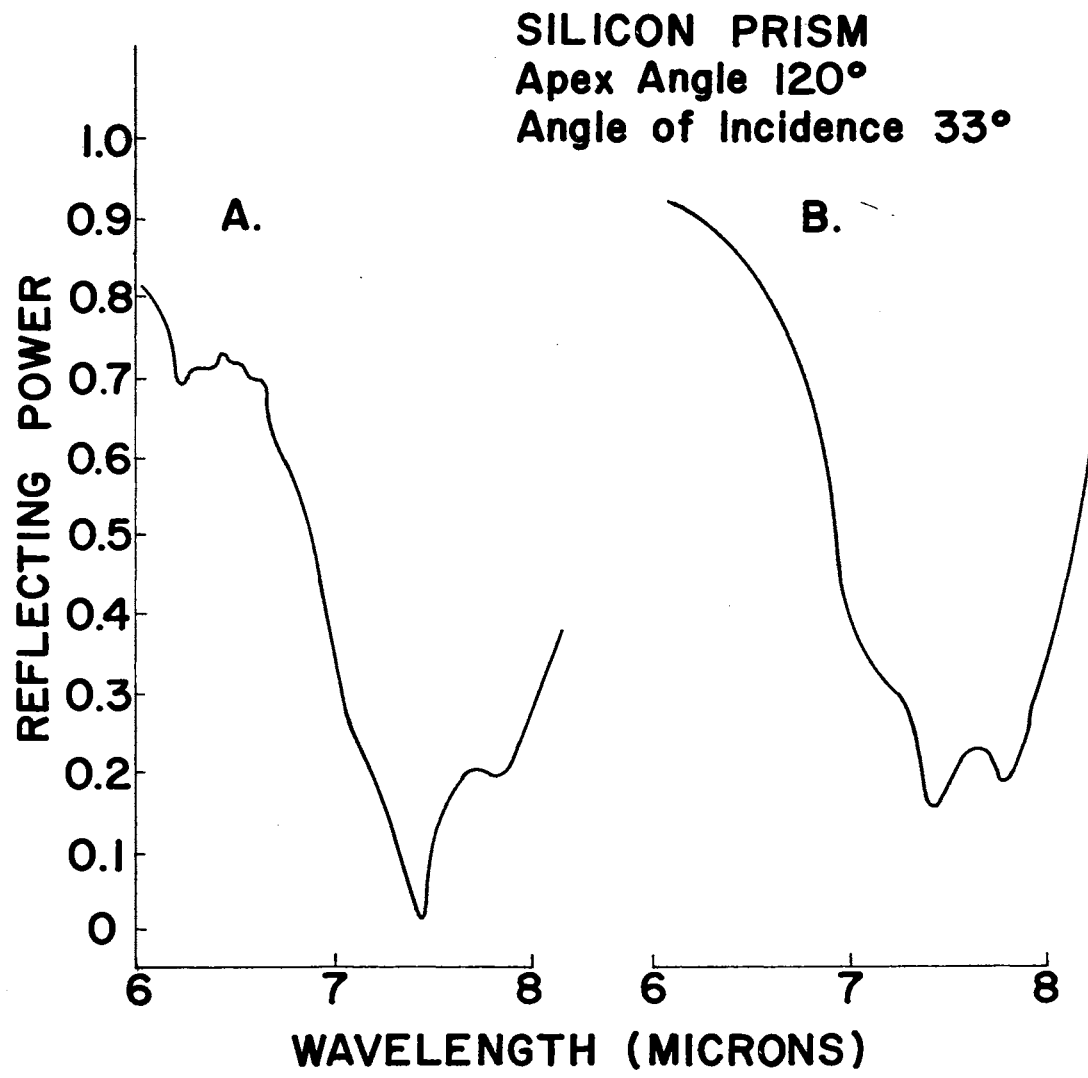


Figure 6. ATR Spectra of Fused LiNO_3

SILICON PRISM
Apex Angle 100°
Angle of Incidence 40°

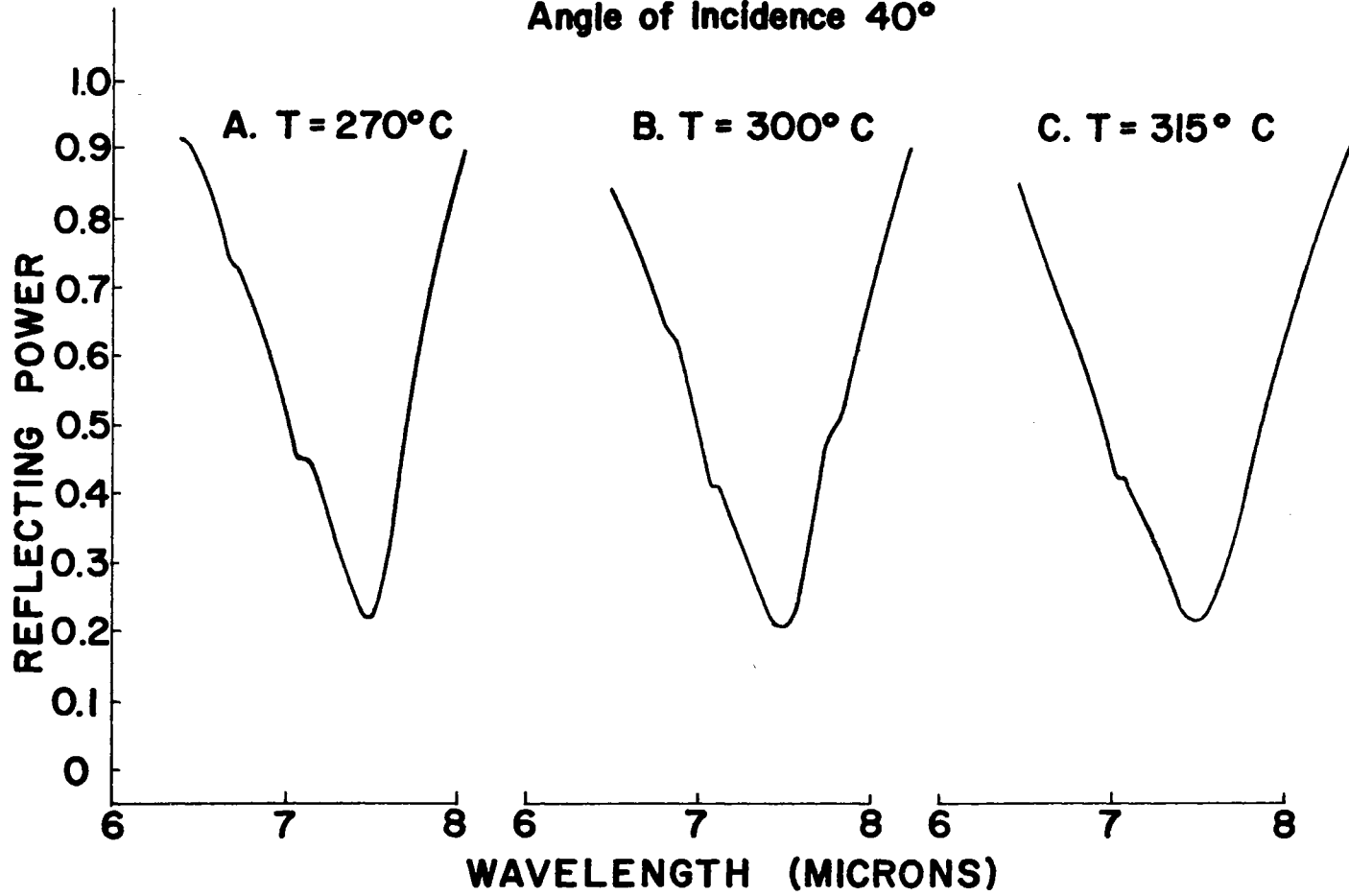
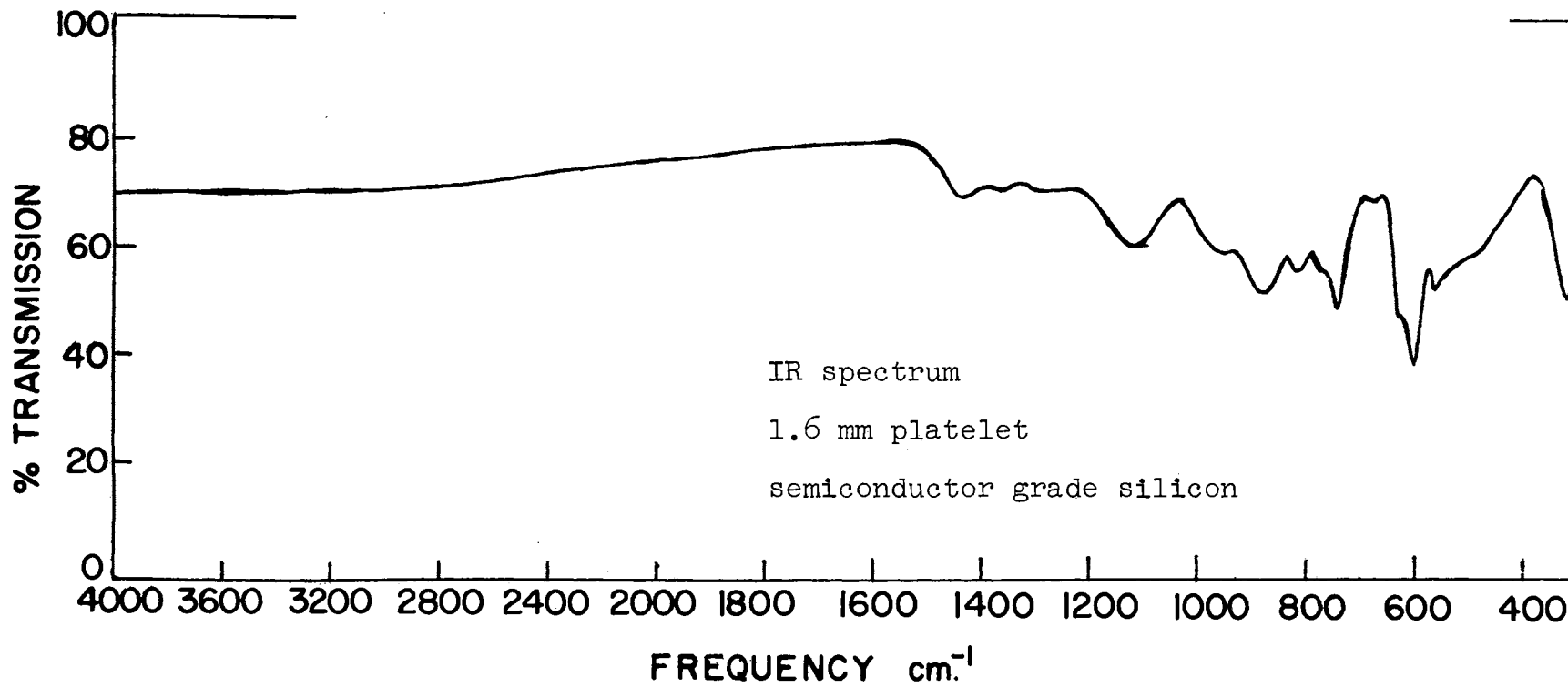


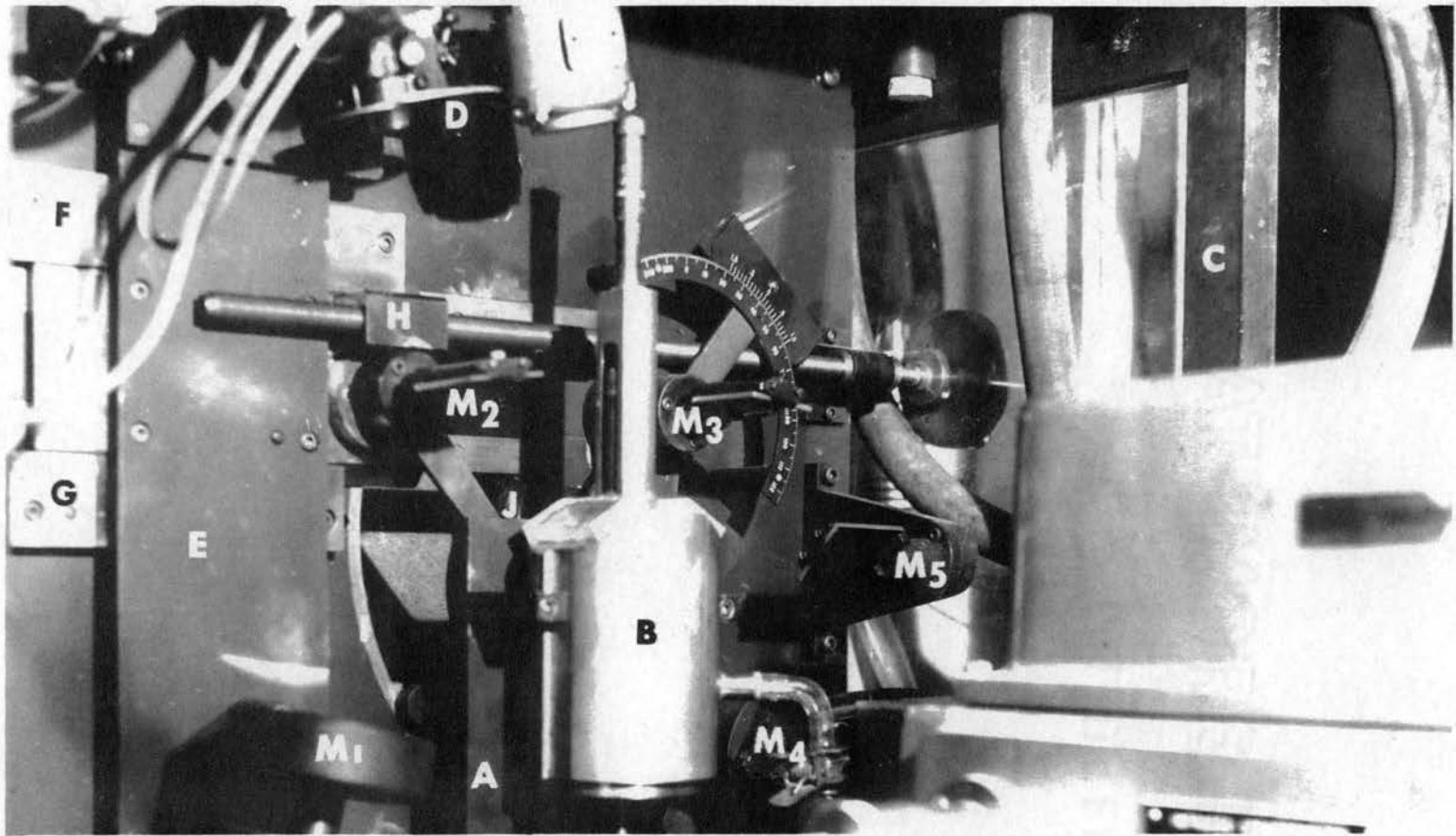
Figure 7. ATR Spectra of Fused LiNO₃

Plate I



I. R. Spectrum of Ultrapure Silicon

Plate II



Foreoptics

BIBLIOGRAPHY

1. W. Bues, Z. physik. Chem. 10, 1 (1957).
2. W. Bues, Z. anorg. u. allgen. Chem. 279, 104 (1955).
3. Bockris, White, and Mackenzie, Physico-Chemical Measurements at High Temperatures, Academic Press, Inc., New York, 1959, ch., W. Bues, "Raman Spectroscopy".
4. J. Greenberg and L. J. Hallgren, Rev. Sci. Instr. 31, 444 (1960).
5. J. K. Wilmschurst and S. Senderoff, J. Chem. Phys., 35, 1070 (1961).
6. T. K. Robinson and W. C. Price, Molecular Spectroscopy, edited by G. Sell, (The Institute of Petroleum, London, 1955), p. 211.
7. P. N. Schatz and Plaskett, J. Chem. Phys. 38, 612 (1963).
8. J. Fahrenfort, Spectrochim. Acta 17, 698 (1961).
9. J. Fahrenfort and Visser, W. M., Spectrochim. Acta 18, 1103 (1962).
10. G. E. Walrafen and D. E. Irish, J. Chem. Phys. 39, 911 (1964).
11. G. J. Janz, T. R. Kozlowski, and S. C. Wait, J. Chem. Phys. 39, 1809 (1963).
12. B. M. Gatehouse, S. E. Livingstone, and R. S. Nyholm, J. Chem. Soc. 1957, 4222.

VITA

Alan Ray Bandy

Candidate for the Degree of

Master of Science

Thesis: APPLICATION OF ATTENUATED TOTAL REFLECTION SPECTROSCOPY TO FUSED
INORGANIC SALTS

Major Field: Physical Chemistry

Biographical:

The author was born near Indianahoma, Oklahoma, on September 13, 1940.

He attended Indianahoma High School for 12 years graduating in 1958.

He attended Cameron State Junior College for 2 years and received a

B.A. in Chemistry in 1964 from Oklahoma State University.